CrossMark

ARTICLE

# Microstructural evolution and functional fatigue of a Ti–25Ta high-temperature shape memory alloy

Hans Jürgen Maier[a] and Elvira Karsten
*Institut für Werkstoffkunde (Materials Science), Leibniz Universität Hannover, Garbsen 30823, Germany*

Alexander Paulsen, Dennis Langenkämper, Peer Decker, Jan Frenzel, Christoph Somsen, Alfred Ludwig, and Gunther Eggeler[c]
*Institut für Werkstoffe, Ruhr-Universität Bochum, Bochum 44780, Germany*

Thomas Niendorf[b]
*Institut für Werkstofftechnik, Universität Kassel, Kassel 34125, Germany*

(Received 5 May 2017; accepted 14 July 2017)

Titanium–tantalum based alloys can demonstrate a martensitic transformation well above 100 °C, which makes them attractive for shape memory applications at elevated temperatures. In addition, they provide for good workability and contain only reasonably priced constituents. The current study presents results from functional fatigue experiments on a binary Ti–25Ta high-temperature shape memory alloy. This material shows a martensitic transformation at about 350 °C along with a transformation strain of 2 pct at a bias stress of 100 MPa. The success of most of the envisaged applications will, however, hinge on the microstructural stability under thermomechanical loading. Thus, light and electron optical microscopy as well X-ray diffraction were used to uncover the mechanisms that dominate functional degradation in different temperature regimes. It is demonstrated the maximum test temperature is the key parameter that governs functional degradation in the thermomechanical fatigue tests. Specifically, ω-phase formation and local decomposition in Ti-rich and Ta-rich areas dominate when $T_{max}$ does not exceed ≈430 °C. As $T_{max}$ is increased, the detrimental phases start to dissolve and functional fatigue can be suppressed. However, when $T_{max}$ reaches ≈620 °C, structural fatigue sets in, and fatigue life is again deteriorated by oxygen-induced crack formation.

## I. INTRODUCTION

There is substantial interest in shape memory alloys (SMAs) that can be operated at elevated temperatures, and SMAs with phase transformation temperatures higher than 100 °C are referred to as high-temperature shape memory alloys (HTSMAs). Still, these materials are only used for niche applications in industry. Today, most of the HTSMAs are based on the nickel–titanium system, where the phase transformation temperature has been shifted up by alloying with ternary elements, such as Pt,[1–5] Pd,[1–4,6] and Hf.[7–11] The current approaches either call for high amounts of expensive noble elements or often result in systems with poor workability.[7,8] It should be noted, however, that for Ni–Ti–Hf HTSMAs the workability issue can be overcome by appropriate processing, and even thin wires can be produced as successfully demonstrated lately.[11]

Lately, titanium–tantalum has been identified as a system that features substantial transformation strains from a martensitic phase transformation occurring at elevated temperature.[12,13] Moreover, Ti–Ta alloys are composed of reasonably priced constituents and demonstrate good workability. The early alloys proposed had a tantalum content of 30–40 at.%. In these alloys, the high-temperature β-phase (bcc) transforms to the low-temperature α″-phase (orthorhombic).[12,14] However, Buenconsejo and co-workers have demonstrated early on that in binary Ti–Ta alloys a hexagonal, so-called ω-phase can form in the temperature regime between 100 and 400 °C.[14,15] The formation of the ω-phase stabilizes the β phase, which in turn results in a loss of the functional properties.[15,16] Thermomechanical loading at elevated temperatures has been reported to speed up functional degradation.[17] Interestingly, a short thermal treatment at 600 °C can be used to dissolve the ω-phase and restore the functional properties.[18,19] Such a heat treatment may, however, not always be possible in actual applications, and thus, other approaches are needed as

Contributing Editor: Yuntian Zhu
Address all correspondence to these authors.
[a]e-mail: maier@iw.uni-hannover.de
[b]e-mail: niendorf@uni-kassel.de
[c]This author was an editor of this journal during the review and decision stage. For the *JMR* policy on review and publication of manuscripts authored by editors, please refer to http://www.mrs.org/editor-manuscripts/.
DOI: 10.1557/jmr.2017.319

 © Materials Research Society 2017 

https://doi.org/10.1557/jmr.2017.319 Published online by Cambridge University Press

well. One is to use ternary systems to delay formation of the ω-phase.[14,20] On the other hand, the phase transformation temperatures are known to increase upon decreasing the tantalum content,[14,20] but the consequences of such an approach on microstructural stability have not be explored yet. Thus, the objective of the present study was to shed light on the phase transformation behavior and the microstructural evolution upon thermomechanical loading in a low tantalum (25 at.%) binary alloy. In fact, as demonstrated in the following, the increase in phase transformation causes a substantial change in damage mechanisms, which makes this alloy substantially different from the previously studied higher tantalum content system. Specifically, an intermediate temperature regime exists for this alloy were functional degradation can be fully suppressed.

## II. MATERIALS AND METHODS

Samples for thermomechanical fatigue tests with a nominal gauge length of 30 mm and a cross section of 2 × 1.5 mm were prepared from polycrystalline Ti–25Ta (in at.%) using electrical discharge machining (EDM). Ti-25Ta block-shaped ingots with a nominal weight of 45 g were prepared by arc melting from high purity raw materials purchased from Hauner Metallische Werkstoffe, Röttenbach, Germany. The ingots were remelted 15 times to ensure good initial chemical homogeneity. For further details on the melting process see Ref. 13. The ingots were then subjected to homogenization annealing at 1100 °C for 25 h under vacuum. This process minimized microscopic heterogeneities that result from dendritic solidification. After annealing, sheets with a final thickness of 2 mm were prepared from the homogenized ingots by rolling. In the first rolling steps, which were conducted after preheating to 800 °C, the thickness of the material was reduced from 17 to 7.7 mm. The average degree of deformation (φ) was close to 0.2. The samples were subjected to an intermediate annealing at 800 °C for 10 min between each two rolling steps. After reaching a thickness of 7.7 mm, the materials were further processed by cold rolling. A final thickness of 2 mm was established after 9 rolling passes, and φ was 0.37 in the last deformation step. Similar to the case of hot rolling, the materials were subjected to intermediate annealing at 800 °C for 10 min between each two cold rolling passes. Finally, fully recrystallized microstructures were obtained after annealing at 900 °C for 10 min followed by water quenching. Further details on thermomechanical treatments are given in Refs. 13 and 21.

Phase transformation temperatures were determined using differential scanning calorimetry (DSC) using a TA instruments DSC2920 cell (TA Instruments, New Castle, Delaware). The DSC tests were carried out in the temperature interval between 20 °C and 620 °C with a heating and cooling rate of 20 °C/min on the recrystallized samples prior to testing. A total of 12 ingots were analyzed by DSC, and the variation between the DSC curves was found to be negligible, which indicates that the process conditions were well controlled. This is important as shape memory behavior is known to be very sensitive to both variations in chemical composition and processing parameters.

The thermomechanical fatigue tests were performed using an electrodynamic test system (MTS Acumen, MTS Systems Corporation, Eden Prairie, Minnesota) equipped with a 3 kN load cell. The samples were conductively heated, and cooling of the samples was realized by compressed air. Temperature in gauge length was measured an Optris PI640 infrared camera (Optris GmbH, Berlin, Germany). Prior to testing, all samples were mechanically ground and polished to remove the EDM-affected surface layer. To check reproducibility of the strain–temperature response, a minimum of five samples were used for each testing condition. The variation in thermomechanical response were found to be negligible, and the strain–temperature curves shown in Figs. 2(a)–2(c) are representative for the given material state.

The microstructural changes induced by the thermomechanical fatigue tests were investigated using optical microscopy, scanning electron microscopy (SEM) and transmission electron microscopy (TEM). For metallography, the specimens were mechanically ground and polished, followed by vibropolishing for 12 h with Eposil M11 (ATM GmbH, Mammelzen, Germany) using a Buehler Vibromet 2 (Buehler, Lake Bluff, Illinois). A Zeiss SUPRA 55VP SEM (Carl Zeiss AG, Oberkochen, Germany), equipped with a Bruker energy dispersive X-ray (EDX) analyzer (Bruker Corporation, Billerica, Massachusetts), was used to characterize the microstructures at higher resolution. The phases present prior to and after the thermomechanical fatigue tests were determined by X-Ray diffraction (XRD) using a Cu $K_\alpha$ source. The TEM analyses were conducted using a Tecnai F20 G2 Supertwin FEG TEM (FEI, Hillsboro, Oregon) operated at 200 kV. The TEM was equipped with an EDX and high angle dark-field detector (HAADF) detector. The TEM foils were prepared using focused ion beam preparation in an FEI Quanta 200 3D Dual Beam SEM (FEI, Hillsboro, Oregon). To analyze the chemical composition of specific locations with high lateral resolution, the HAADF detector was used in combination with the scanning transmission electron microscope (STEM) mode. Bright-field, high-resolution TEM and fast Fourier transform patterns were used for local microstructural characterizations.

https://doi.org/10.1557/jmr.2017.319 Published online by Cambridge University Press

## III. RESULTS AND DISCUSSION

The DSC curve in Fig. 1 represents the first transformation cycle of the sheet material. The phase transformation temperatures for the cooling and first heating peak determined fit with those expected based on the literature.[12,14,22] Interestingly, there is a clear sign for another transformation (peaks beyond 520 °C). It is well known that there can be a so-called "first cycle effect".[23] However, this is not very likely in the present case as the dislocations which could provide for such an effect should have been essentially wiped out by the final 900 °C recrystallization treatment. Thus, this additional peak might indicate a potential lack of microstructural stability instead. In fact, it is well known that the β-phase is not stable in the temperature range from 250 °C to 600 °C.[24] Specifically, the formation of the ω-phase has been reported to occur between 100 °C and 400 °C, which in turn results in functional degradation.[15,17,24] At temperatures exceeding 400 °C, the α-phase can form as well.[24–26]

To shed light on the relationship between the microstructural changes and functional behavior, thermomechanical fatigue tests were performed in three different temperature intervals. The first one (40–430 °C) covered the regime were the ω-phase might form. The second interval (40–520 °C) was chosen to include the extra peak seen in the DSC data (Fig. 1). The third set of tests spanned the range from 40 °C to 620 °C to allow for dissolution of the ω-phase. In each case, the initial transformation strain under a superimposed stress of 100 MPa was about 2 pct (Fig. 2). This is higher than the value (1.3 pct) reported previously for Ti–30Ta,[17–19] which might indicate easier microstructural rearrangement. Moreover, the phase transformation is occurring at higher temperature than in Ti–30Ta (Ms = 173 °C, Af = 250 °C)[27] due to the lower tantalum content. Obviously, this would make the material more attractive for the envisaged elevated temperature applications. However, compared to Ti–30Ta,[19] the Ti–25Ta alloy displays more rapid functional degradation [Fig. 2(a)] in the low maximum temperature tests.

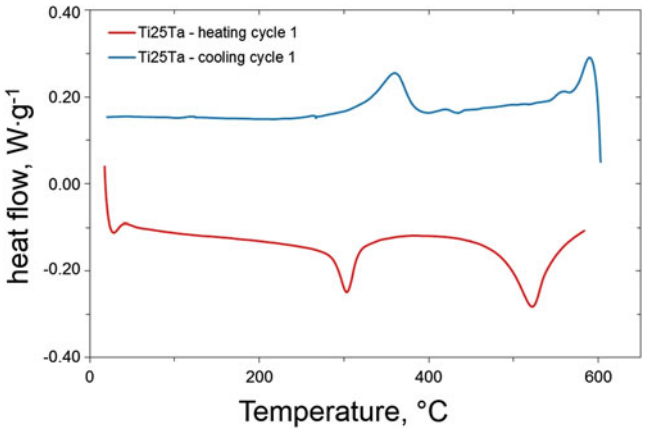



FIG. 1. DSC charts at heating and cooling rates of 20 °C/min for recrystallized Ti–25Ta prior to thermomechanical cycling.

Figure 2 also demonstrates that the strain–temperature response in the three different temperature ranges used is substantially different. In case of a maximum temperature of 430 °C [Fig. 2(a)], the rapid functional degradation is prominent, and transformation is reduced to about 0.5 pct after just 50 cycles. There is also a quite pronounced shift of transformation temperatures toward lower temperatures. As it is well known, the phase transformation temperatures decrease with increasing tantalum content[12]; this hints at a change in chemical composition of the transformation matrix. Specifically, the formation of a titanium-rich α-Ti-phase, which itself does not show a martensitic transformation, would result in an increase in tantalum content of the matrix and the observed shift in the macroscopically observed phase transformation temperature. In fact, the formation of a α-Ti-phase in Ti–Ta alloys has been reported earlier,[17,21] and Albrecht et al.[28] have shown that α-Ti-phase forms under tensile stresses in β-Ti alloys at temperatures around 400 °C. At the same time, formation of the ω-phase in the austenite is expected in the temperature range from 100 °C to 400 °C.[12,14]

At first glance, one would expect that with increasing maximum temperature, microstructural instability increases, and thus, functional degradation should occur more rapidly. However, as demonstrated in Fig. 2(b), the change in stress-temperature response with the number of cycles is substantially less pronounced. Moreover, the hysteresis curves essentially change on the high-temperature side in Fig. 2(b). In other words, functional degradation now occurs predominantly in the austenitic phase. This can be partly attributed to enhanced dislocation activity in the high-temperature part of the test. Recent studies on Ti–30Ta have already demonstrated substantial dislocation activity to occur at temperatures as low as 400 °C in thermomechanical tests.[17] This not only affects strain–temperature hysteresis[29,30] but could trigger a decomposition into Ti-rich and Ta-rich regions. This would explain the shift of the degradation to the high-temperature side but not obvious retardation of the degradation kinetics. In this context, one should recall that the maximum temperature of the tests shown in Fig. 2(b), coincides with the extra peak seen in the DSC chart (Fig. 1). Moreover, Fig. 2(b) indicates that despite the substantial decrease in transformation strain during cycling, the associated transformation temperature hardly change at all. An explanation would be (partial) dissolution of the α- and/or the ω-phase, such that the matrix returns to its initial chemical composition. Alternatively, the increase in dislocation density could result in an increase in elastic strain energy.[29–32] This effect could stabilize transformation temperatures despite the change

https://doi.org/10.1557/jmr.2017.319 Published online by Cambridge University Press

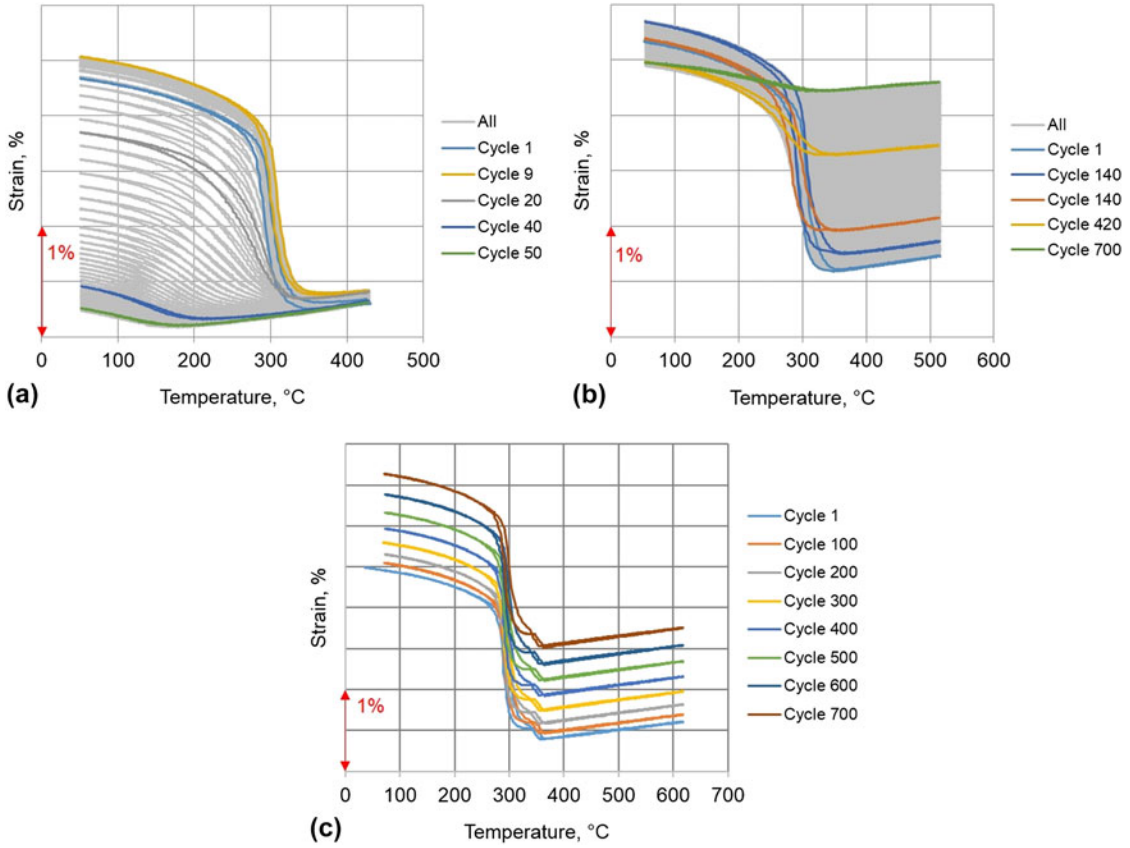



FIG. 2. Strain–temperature curves obtained for Ti–25Ta during thermomechanical cycling with heating and cooling rates of 20 °C/s at 100 MPa between (a) 40–430 °C, (b) 40–520 °C, and (c) 40–620 °C; in the latter case, the superimposed stress was reduced to 0 MPa in the austenitic regime, see main text for details.

in chemical composition of the matrix as suggested for Ti–30Ta earlier.[17]

To avoid excessive plastic deformation in the high-temperature part of the curve, the thermomechanical experiments with a maximum temperature of 620 °C [Fig. 2(c)] were conducted in a slightly different way. The tests were started with a superimposed stress of 100 MPa. As soon as the transformation from martensite to austenite had occurred, the stress was reduced to 0 MPa within 1 s while heating continued up to 620 °C. Upon cooling, the stress of 100 MPa was reapplied shortly before the onset of the back transformation. In curves shown in Fig. 2(c), this unloading and reloading results in the little extra hump around 350 °C. Interestingly, there is only an upward shift of the hysteresis loops, but the overall transformation strain of about 2 pct remained constant. For sake of comparison with the data in Fig. 2(b), only the first 700 cycles are shown in Fig. 2(c). However, transformation strain did not change significantly up to 2000 cycles, when the sample finally failed by structural fatigue (cyclic crack growth).

As the high maximum temperature of 620 °C was chosen based on the second peak position in the DSC chart (Fig. 1), it can be assumed that the constant transformation strain seen in the thermomechanical fatigue tests [Fig. 2(c)] indicates that the ω- and/or the Ti-rich α-phase get dissolved during the high-temperature part of the curve. At least for Ti–30Ta it was shown earlier that a short high-temperature excursion suffices to dissolve the ω-phase.[18,19] The slight shift of the transformation temperature toward higher values [Fig. 2(c)] can be attributed to formation of Ta-rich phases which affects the matrix composition and thus, the corresponding phase transformation temperature.[12,20,33]

To better separate the individual contributions to the overall macroscopic change in strain–temperature response, the microstructures present after thermomechanical fatigue were characterized by XRD and electron microscopy. Figure 3 shows XRD data obtained from the thermomechanically fatigued samples. In case of the low maximum temperature test [430 °C, Fig. 2(a)], the X-ray diffractogram shows the presence of the α″-phase and the α-phase. As the latter is Ti-rich,[21] the tantalum content in the bulk increases and the phase transformation temperatures are shifted to lower values [Fig. 2(a)]. The ω-phase is not seen in Fig. 3(a), but hard to detect by XRD as the precipitates are very fine.[19] Thus, the presence of the ω-phase cannot be excluded. Formation of the ω-phase

https://doi.org/10.1557/jmr.2017.319 Published online by Cambridge University Press

has been discussed as an important contribution to the decrease in phase transformation temperature.[12,19] In fact, for Ti–30Ta thermomechanically cycled between 40 °C and 400 °C, only the formation of the ω-phase was reported but no α-phase. This can be explained based on the difference in Ta content. Tantalum shows some solubility in the α-phase[34,35] but is a β-stabilizer.[34,36] Hence, the higher the tantalum content, the less probable is the formation the α-phase, and Ti–25Ta (α- and ω-phase formation) and Ti–30Ta (ω-phase formation only) become quite different in this respect.

The XRD data shown in Fig. 3(b) demonstrate that both the α-phase and the α″-phase were still present after the thermomechanical test conducted with higher maximum temperature of 520 °C [Fig. 2(b)]. However, the α-phase content is lowered, which indicates that part of the α-phase has been dissolved during the high-temperature part of the test, which explains the lower functional degradation rate in this case [see Figs. 2(a) and 2(b)].

The TEM studies substantiated the above interpretations and provided further insight. The EDX analysis [Fig. 4(a)] clearly demonstrated the presence of Ti-rich phases. In addition, there are bright appearing, Ta-rich β-phases (bcc), which are known to form preferentially at grain boundaries.[21,27] Because of the small size and low volume fraction, these are not captured in the XRD data [Fig. 3(a)]. By contrast, the needle-like Ti-rich α-phase which is seen within the grains (Fig. 4) is already detectable by XRD [Fig. 3(a)]. Thus, functional degradation under these conditions appears to be governed by β-phase formation at the grain boundaries and needle-like α-phase within the grains.

The material contrast used for the back-scattered electron image in Fig. 5 clearly demonstrates the decomposition in the Ti-rich α-phase (darker) and the Ta-rich β-Ta phase (brighter). In addition, fine needle-like precipitates are apparent within the grains. In creep tests conducted on Ti–30Ta, similarly appearing precipitates

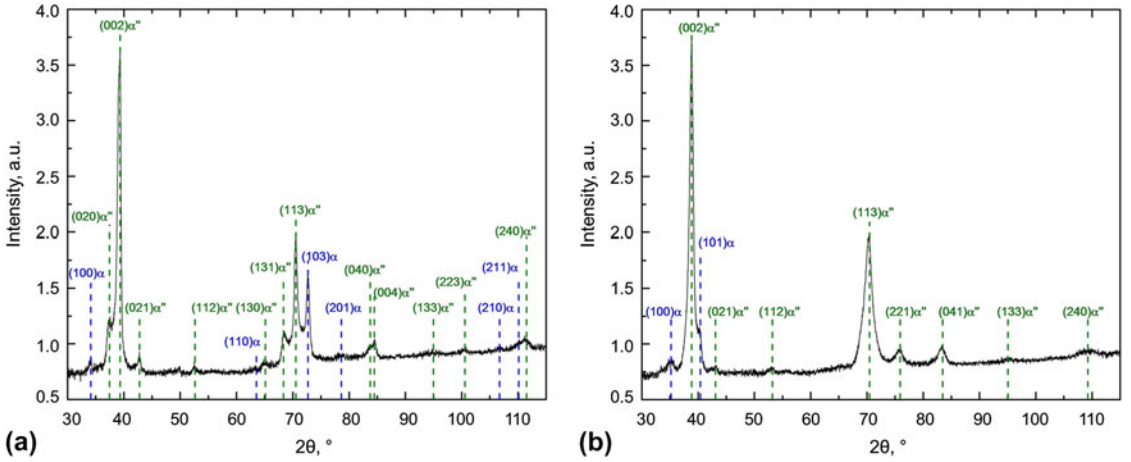



FIG. 3. XRD profiles showing relative intensities at room temperature for Ti–25Ta (a) after a thermomechanical fatigue test conducted at 100 MPa between (a) 40 °C and 430 °C and (b) 40 °C and 520 °C; heating and cooling rates were 20 °C/s.

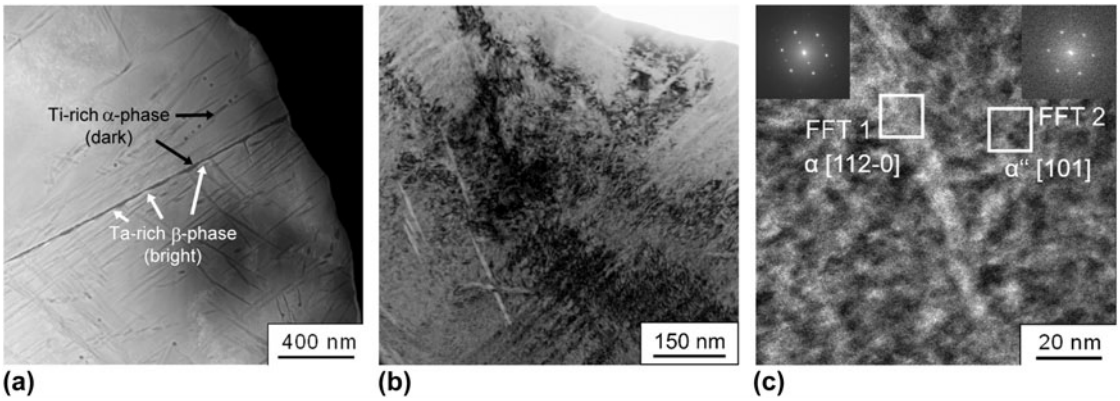



FIG. 4. TEM images of Ti–25Ta after thermo-mechanical cycling between 40–430 °C under a superimposed stress of 100 MPa: (a) HAADF STEM image, (b) bright-field image, and (c) two times filtered high resolution detail showing the needle-like precipitation (α-phase) and the surrounding matrix (α″-phase).



https://doi.org/10.1557/jmr.2017.319 Published online by Cambridge University Press

have been observed for tests conducted at 500 °C and 120 MPa, i.e., test parameters close to the one used for thermomechanical experiments in the present study. These precipitates were identified as Ti-rich β-Ti,[21,27] which can transform back to α″-martensite. However, the transformation temperatures would be very high, as this phase contains little tantalum. Thus, the Ti-rich β-Ti will be essentially retained upon cooling to 40 °C, which in turn results in loss of transformation strain. The overall kinetics of the process are, however, slower than in the 40–430 °C test.

The TEM analysis of the sample thermomechanically fatigued between 40 °C and 520 °C also demonstrated the presence of the ω-phase. This phase is very small and hard to see in bright-field images. In annular dark-field mode, the contrast is improved [Fig. 6(a)] and the selected area diffraction pattern [Fig. 6(b)] clearly demonstrate the extra reflections from the ω-phase that has precipitated [Fig. 6(c)] with the β-matrix. This process hinders back transformation, and thus, functional degradation sets in. Moreover, the presence (and dissolution) of the ω-phase seems to fit with the extra peak observed in the DSC curves (Fig. 1). This rationale, however, requires additional microstructural studies.

In a previous study on Ti–30Ta, it has been demonstrated that a short heat treatment at 600 °C allows for a dissolution of the ω-phase.[18,19] Based on the data shown in Fig. 6, the maximum temperature of 520 °C is not high enough to provide for this effect in the thermomechanical fatigue tests conducted on Ti–25Ta. Thus, functional degradation in Ti–25Ta for the 40–520 °C case can be attributed to the combined effects of α-Ti-phase and β-Ta-phase formation at the grain boundaries, precipitation of needle-like β-Ti-phase within the grains along with formation of ω-phase and enhanced dislocation activity in the high-temperature part of the test.

As demonstrated in Fig. 2(c), structural degradation is pronounced in the thermomechanical fatigue tests conducted on Ti–25Ta in the temperature range between 40 °C and 620 °C. In fact, the material failed by conventional fatigue crack nucleation and propagation. This substantial difference in behavior to the tests conducted with lower maximum test temperatures is again rooted in microstructure. In this case, the XRD data were not revealing accurate phase information as the peaks of the β- and α-phase almost coincide in the interesting regime for this alloy.[27] However, the SEM images shown in Fig. 7 clearly demonstrate that decomposition in Ti-rich [Fig. 7(b)] and Ta-rich [Fig. 7(c)] phases occur under these conditions as well. Given the higher maximum temperature, it is understandable that the effect is more pronounced than in the other test. More importantly, the decomposition clearly has started at the grain boundaries and triple points [Fig. 7(a)]. EDX analysis demonstrated up to 93 at.% Ti for the regions appearing dark in the SEM images and up to 36 at.% Ta for the bright ones. As the material still displayed an almost unchanged transformation strain after 700 cycles [Fig. 2(c)], it can be assumed that the material is

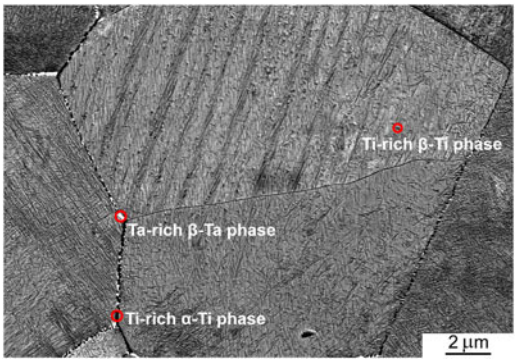



FIG. 5. Back-scattered electron image of Ti–25Ta after thermomechanical cycling between 40–520 °C under superimposed stress of 100 MPa with heating and cooling rates of 20 °C/s.

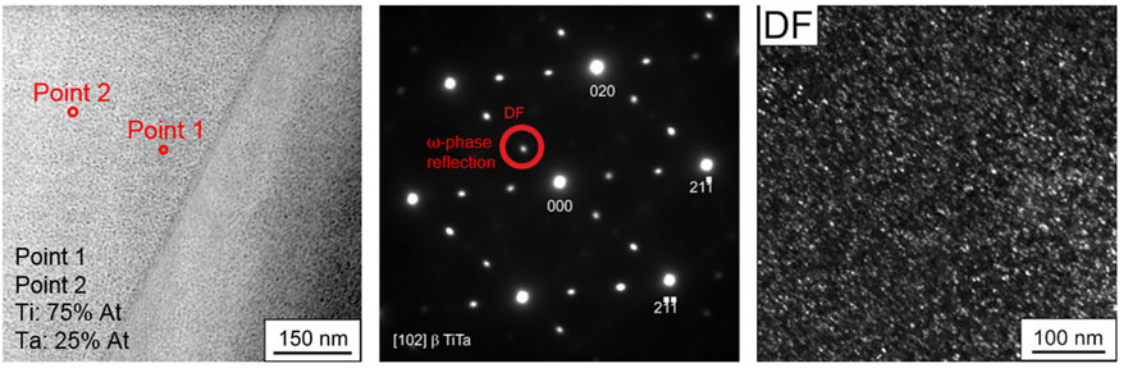



FIG. 6. TEM images of Ti–25Ta after thermomechanical cycling between 40 °C and 520 °C under a superimposed stress of 100 MPa: (a) annular dark-field image in STEM mode, (b) selected area diffraction pattern for [102]β TiTa showing reflections from the ω-phase, and (c) corresponding dark-field image.

https://doi.org/10.1557/jmr.2017.319 Published online by Cambridge University Press

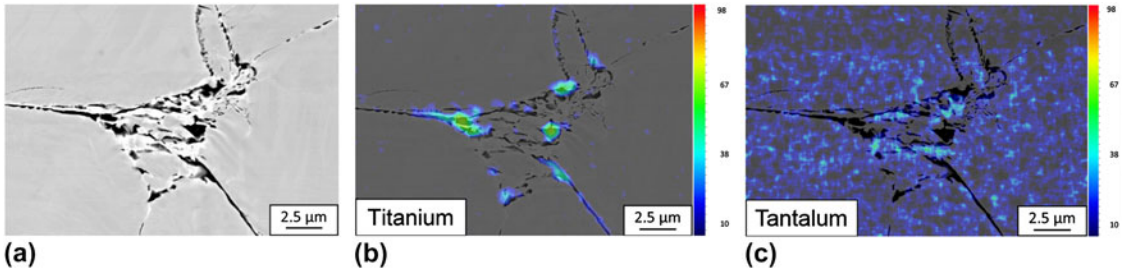



FIG. 7. SEM images of Ti–25Ta after thermomechanical cycling between 40 °C and 620 °C under a superimposed stress of 100 MPa: (a) back-scattered electron image and corresponding elemental distribution map for (b) titanium and (c) tantalum.

essentially austenitic in the high-temperature part of cycle, but with locally Ti-rich and Ta-rich regions. In fact, EDX analysis revealed areas with a composition of Ti–25Ta, which explains the slight increase in transformation temperature seen upon cycling [Fig. 2(c)].

Upon cooling, the chemical heterogeneity of the austenite results in the martensitic transformation to α″ with locally different Ti and Ta content. If the Ti content gets high enough, the transformation might get suppressed locally, and some of the Ti-rich phases seen at the grain boundaries should have formed this way.

As seen in Fig. 2(c), the upward shift in the hysteresis loops is small initially and then increases significantly. This shift is essentially due to conventional fatigue crack formation. These cracks started at the surface and propagated within the grains (not shown here). This indicates that the local decomposition observed at the grain boundaries (Fig. 7) does not play a significant role in this context. It is well known that Ti–Ta alloys are prone to high-temperature oxidation,[37] and it appears that the oxidation-induced crack formation dominates in this case.

As detailed above, the microstructural evolution is quite complex in this system. Thus, the effect of temperature test regime on microstructural evolution along with the resulting changes in macroscopic strain–temperature response has been summarized in the schematic shown in Fig. 8. To ease interpretation a schematic DSC chart along with the key temperature regimes is shown in Fig. 8(a).

In each experiment, the test started with the material being in the martensitic state (marked by A in Fig. 8). Upon heating, the ω-phase is formed. The relevant temperature range for this process in Ti–Ta alloy is about 100–400 °C.[12,14] Starting at around 400 °C, α-phase formation sets in both at grain boundaries an in the grain interiors. In parallel to this Ti-rich phase, the Ta-rich β-phase forms at grain boundaries. Thus, at point B in Fig. 8(b), the bulk of the alloy is in the austenitic state, but there is ω-phase and α-phase in the grain interiors and α-phase and Ta-rich β-phase at the grain boundaries. For Ti–Zr alloys it has been reported that the α- and β-phase observed at the grain boundaries form by "consuming" β and ω.[15] A similar process might occur in Ti–25Ta as

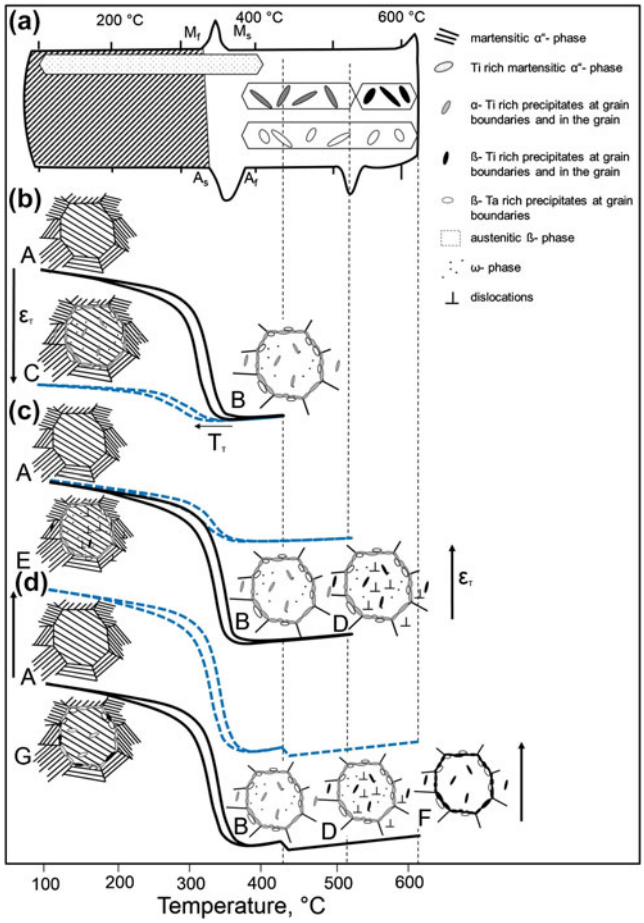



FIG. 8. Schematic illustration of microstructural evolution that result in functional degradation of Ti–25Ta during thermomechanical cycling; (a) schematic DSC chart including the key microstructural features, (b), (c) and (d): corresponding strain-temperature hysteresis loops; see main text for details.

well. In fact, the formation of the α-phase upon dissolution of the ω-phase has been observed in Ti–30Ta upon heat treatment. Similarly, α-phase formation from ω-phase has been reported for Ti–Mo and Ti–Nb.[26]

Upon cooling from 430 °C (point B), the detrimental phases ω, α-Ti, and β-Ta remain, and as the process is cyclically repeated, their volume fraction increases and rapid functional degradation sets in [point C in Fig. 8(b)].

https://doi.org/10.1557/jmr.2017.319 Published online by Cambridge University Press

As discussed above, the changes in matrix composition also cause a slight shift toward lower transformation temperatures as marked by the arrow in Fig. 8(b).

In case of the tests conducted up to the higher temperature of 520 °C [point D in Fig. 8(c)], the α-phase starts to transform to Ti-rich β. This process sets in around 500 °C in the grain interior and at about 520 °C also at the grain boundaries, and corresponds to the second peak in the DSC chart. This process appears to be mainly driven by temperature but not by cycling, as it has been reported for creep tests performed under similar test conditions.[21,27] Because of the combination of high temperature and superimposed stress, dislocation activity is enhanced as well. During cooling from point D, the ω-phase, the β-Ta, and α-Ti-phase at the grain boundaries and the dislocations all remain in the microstructure. Depending on their actual chemical composition the β-Ti precipitates in the grain interiors can transform to martensite or remain as well [point E in Fig. 8(c)]. As detailed above, these processes also result in functional degradation, but this time the effect is more pronounced on the high-temperature side of the loop [marked by $\varepsilon_T$ in Fig. 8(c)].

The behavior in the modified test, where the external stress was not present in the high-temperature part of the cycle to curtail excessive plastic deformation, is sketched in Fig. 8(d). On heating, the detrimental ω-phase gets dissolved again and the α-Ti-phase transforms (partly) to β-Ti. In addition, dislocations can annihilate or rearrange. Upon cooling, the austenitic matrix, Ti-rich β-phase within the grain and at the grain boundaries and the β-Ta phase at the grain boundaries can all transform back to martensite. Depending on actual chemical composition, part of these may locally not transform. This effect is, however, only minor, and thus, functional degradation is not a key issue in this case. Given the high maximum temperature, oxidation becomes relevant instead and structural fatigue starts to govern fatigue life. As indicated by the arrows in Fig. 8(d), crack opening macroscopically results in an upward shift of the hysteresis loops.

Apparently, functional degradation can be minimized by appropriate temperature-time-profiles, but the high-temperature excursions needed will limit fatigue life. In case of the test shown in Fig. 8(d), the samples did not fail before 2000 cycles. As this will not suffice for many of the envisaged applications, research is underway to address oxidation behavior.

## IV. CONCLUSIONS

The functional fatigue behavior of a Ti–25Ta shape memory alloy was studied under thermomechanical loading in different temperature regimes. The main results can be summarized as follows:

(1) The material shows a martensitic transformation at elevated temperatures (≈350 °C) with substantial transformation strain (≈2 pct) under a superimposed stress of 100 MPa.

(2) Functional degradation behavior does vary substantially with the maximum test temperature used in the thermomechanical test. For lower maximum test temperatures ($T_{max} \approx 430$ °C), formation of the ω-phase and local decomposition in Ti-rich and Ta-rich areas along with α-Ti formation are the dominant processes.

(3) As $T_{max}$ is increased further, the detrimental phases start to dissolve and functional behavior can be almost fully suppressed in thermomechanical test when $T_{max}$ substantially exceeds 520 °C as long as dislocation activity in the high-temperature part is not excessive.

(4) In thermomechanical fatigue tests with a $T_{max}$ of 620 °C, functional degradation could be essentially suppressed, but the samples finally failed beyond 2000 cycles by structural fatigue due to oxidation-induced crack formation.

## ACKNOWLEDGMENT

Financial support by Deutsche Forschungsgemeinschaft within the Research Unit Program "Hochtemperatur-Formgedächtnislegierungen" (Contract nos. MA1175/34-2, LU1175/11-2, and NI1327/2-2) is gratefully acknowledged.

## REFERENCES

1. K. Otsuka and X. Ren: Recent developments in the research of shape memory alloys. *Intermetallics* **7**(5), 511 (1999).
2. J. Ma, I. Karaman, and R.D. Noebe: High temperature shape memory alloys. *Int. Mater. Rev.* **55**(5), 257 (2010).
3. P.G. Lindquist and C.M. Wayman: Shape memory and transformation behavior of martensitic Ti–Pd–Ni and Ti–Pt–Ni alloys. In *Engineering Aspects of Shape Memory Alloys*, T.W. Duerig, K.N. Melton, D. Stöckel, and C.M. Wayman, eds. (Butterworth-Heinemann, London, Boston, Singapore, Sydney, Toronto, Wellington, 1990); p. 58.
4. J. Van Humbeeck: High temperature shape memory alloys. *J. Eng. Mater. Technol.* **121**(1), 98 (1999).
5. R. Noebe, D. Gaydosh, S. Padula, II, A. Garg, T. Biles, M. Nathal, and W.D. Armstrong: Properties and potential of two (Ni, Pt) Ti alloys for use as high-temperature actuator materials. *Smart Mater. Struct.* **5761**, 364 (2005).
6. K.C. Atli, I. Karaman, and R.D. Noebe: Influence of tantalum additions on the microstructure and shape memory response of $Ti_{50.5}Ni_{24}Pd_{25}$ high-temperature shape memory alloy. *Mater. Sci. Eng., A* **613**, 250 (2014).
7. X.L. Meng, Y.F. Zheng, W. Cai, and L.C. Zhao: Two-way shape memory effect of a TiNiHf high temperature shape memory alloy. *J. Alloys Compd.* **372**(1–2), 180 (2004).
8. S. Besseghini, E. Villa, and A. Tuissi: Ni–Ti–Hf shape memory alloy: Effect of aging and thermal cycling. *Mater. Sci. Eng., A* **273**, 390 (1999).
9. S.M. Saghaian, H.E. Karaca, M. Souri, A.S. Turabi, and R.D. Noebe: Tensile shape memory behavior of $Ni_{50.3}Ti_{29.7}Hf_{20}$ high temperature shape memory alloys. *Mater. Des.* **101**, 340 (2016).

https://doi.org/10.1557/jmr.2017.319 Published online by Cambridge University Press

10. S.M. Saghaian, H.E. Karaca, H. Tobe, M. Souri, R. Noebe, and Y.I. Chumlyakov: Effects of aging on the shape memory behavior of Ni-rich $Ni_{50.3}Ti_{29.7}Hf_{20}$ single crystals. *Acta Mater.* **87**, 128 (2015).
11. D. Canadinc, W. Trehern, H. Oscan, C. Hayrettin, O. Karakoc, I. Karaman, F. Sun, and Z. Chaudhry: On the deformation response and cyclic stability of $Ni_{50}Ti_{35}Hf_{15}$ high temperature shape memory alloy wires. *Scr. Mater.* **135**, 92 (2017).
12. P.J.S. Buenconsejo, H.Y. Kim, H. Hosoda, and S. Miyazaki: Shape memory behavior of Ti–Ta and its potential as a high-temperature shape memory alloy. *Acta Mater.* **57**(4), 1068 (2009).
13. J. Zhang, R. Rynko, J. Frenzel, C. Somsen, and G. Eggeler: Ingot metallurgy and microstructural characterization of Ti–Ta alloys. *Int. J. Mater. Res.* **105**, 156 (2014).
14. P.J.S. Buenconsejo: Development and characterization of Ti–Ni based and Ti–Ta based shape memory alloys for novel applications. Ph.D. thesis, University of Tsukuba, Japan, 2009.
15. B.S. Hickman: The formation of omega phase in titanium and zirconium alloys: A review. *J. Mater. Sci.* **4**, 554 (1969).
16. J.L. Murray: The Ta–Ti (tantalum–titanium) system. *Bull. Alloy Phase Diagrams* **2**(1), 62 (1981).
17. T. Niendorf, P. Krooß, C. Somsen, R. Rynko, A. Paulsen, E. Batyrshina, J. Frenzel, G. Eggeler, and H.J. Maier: Cyclic degradation of titanium–tantalum high-temperature shape memory alloys—The role of dislocation activity and chemical decomposition. *Funct. Mater. Lett.* **8**, 1550062 (2015).
18. T. Niendorf, P. Krooß, E. Batyrsina, A. Paulsen, Y. Motemani, A. Ludwig, P. Buenconsejo, J. Frenzel, G. Eggeler, and H.J. Maier: Functional and structural fatigue of titanium tantalum high temperature shape memory alloys (HTSMAs). *Mater. Sci. Eng., A* **620**, 359 (2015).
19. T. Niendorf, P. Krooß, E. Batyrsina, A. Paulsen, J. Frenzel, G. Eggeler, and H.J. Maier: On the functional degradation of binary titanium–tantalum high-temperature shape memory alloys—A new concept for fatigue life extension. *Funct. Mater. Lett.* **7**, 1450042 (2014).
20. P.J.S. Buenconsejo, H.Y. Kim, and S. Miyazaki: Novel β-TiTaAl alloys with excellent cold workability and a stable high-temperature shape memory effect. *Scr. Mater.* **64**, 1114 (2011).
21. R. Rynko, A. Marquardt, A. Paulsen, J. Frenzel, C. Somsen, and G. Eggeler: Microstructural evolution in a Ti–Ta high-temperature shape memory alloy during creep. *Int. J. Mater. Res.* **106**, 331 (2015).
22. H.Y. Kim, T. Fukushima, P.J. Buenconsejo, T. Nam, and S. Miyazaki: Martensitic transformation and shape memory properties of Ti–Ta–Sn high temperature shape memory alloys. *Mater. Sci. Eng., A* **528**, 7238 (2011).
23. W. Siegert, K. Neuking, M. Mertmann, and G. Eggeler: First cycle shape memory effect in the ternary NiTiNb system. *J. Phys.* **112**, 739 (2003).
24. T.B. Massalski, H. Okamato, P.R. Subramanian, and L. Kacprzak: *Phasen-Diagramm Ti–Ta, Binary Alloys Phase Diagrams* (ASM International, Metals Park, Ohio, 1990).
25. J.C. Williams, B.S. Hickman, and D.H. Leslie: The effect of ternary additions on the decomposition of metastable beta-phase Ti alloys. *Metall. Trans.* **2**, 477 (1971).
26. B.S. Hickman: Omega phase precipitation in alloys of titanium with transition metals. *Trans. Metall. Soc. AIME* **245**, 1329 (1969).
27. R. Rynko: Mikrostrukturelle Untersuchungen von thermisch und thermomechanisch induzierten Strukturbildungsprozessen in Ti–Ta Hochtemperatur-Formgedächtnislegierungen. Ph.D. thesis, Ruhr-Universität Bochum, Bochum, Germany, 2015.
28. J. Albrecht, T. Duering, and D. Richter: Verfahren zur Herstellung eines Bauteils aus einer Titanlegierung, sowie Bauteil und Verwendung des Bauteils. Europäische Patentanmeldung Patent Number 0062365, 7, 1982.
29. K.C. Atli, I. Karaman, R.D. Noebe, and D. Gaydosh: The effect of training on two-way shape memory effect of binary NiTi and NiTi based ternary high temperature shape memory alloys. *Mater. Sci. Eng., A* **560**, 653 (2013).
30. J. Dadda, H.J. Maier, I. Karaman, and Y. Chumlyakov: High-temperature *in situ* microscopy during stress-induced phase transformations in $Co_{49}Ni_{21}Ga_{30}$ shape memory alloy single crystals. *Int. J. Mater. Res.* **101**, 1503 (2010).
31. J. Dadda, H.J. Maier, I. Karaman, and Y.I. Chumlyakov: Cyclic deformation and austenite stabilization in $Co_{35}Ni_{35}Al_{30}$ single crystalline high-temperature shape memory alloys. *Acta Mater.* **57**, 6123 (2009).
32. Ch. Grossmann, J. Frenzel, V. Sampath, T. Depka, and G. Eggeler: Elementary transformation and deformation processes and the cyclic stability of NiTi and NiTiCu shape memory spring actuators. *Metall. Mater. Trans. A* **40**, 2530 (2009).
33. Y. Al-Zain, Y. Sato, H.Y. Kim, H. Hosoda, T.H. Nam, and S. Miyazaki: Room temperature aging behavior of Ti–Nb–Mo-based superelastic alloys. *Acta Mater.* **60**, 2437 (2012).
34. M. Peters, J. Hemptenmacher, J. Kumpfert, and C. Leyens: Titan und Titanlegierungen: Struktur, Gefüge, Eigenschaften. In *Titan und Titanlegierungen*, M. Peters and C. Leyens, eds. (WILEY-VCH Verlag GmbH & Co. KGaA, Weinheim, 2002); p. 1.
35. R. Boyer, G. Welsch, and E.W. Collings: *Materials Properties Handbook: Titanium Alloys* (ASM International, Materials Park, OH, 1994).
36. T.R. Bieler, R.M. Trevino, and L. Zeng: Alloys: Titanium. In F. Bassani, G.L. Liedl, and P. Wyder, eds., *Encyclopedia of Condensed Matter Physics* (Elsevier, 2005); p. 65.
37. R.F. Vojtovich and Eh.I. Golovko: Oxidation of Ti–Ta and Ti–Nb alloys. *Izv. Akad. Nauk SSSR, Met.* **1**, 222 (1979).


https://doi.org/10.1557/jmr.2017.319 Published online by Cambridge University Press